

Delft University of Technology

Faculty of Mechanical Engineering, Maritime Technology & Technical Materials Sciences  
(3mE)



**Master Thesis**

submitted for the degree of

**Master of Science**

**Vestibular contribution to balance control during a sit-to-walk task**

by

Katla Kristín Guðmundsdóttir  
5473098

Submission Date: October 20, 2023

Supervisors: Eline van der Kruk  
Patrick Forbes



## CONTENTS

<b>I</b>	<b>Introduction</b>	4
<b>II</b>	<b>Methods</b>	5
II-A	Subjects . . . . .	5
II-B	Protocol . . . . .	5
II-C	Stimulus . . . . .	5
II-D	Instrumentation . . . . .	5
II-E	Analysis . . . . .	6
II-F	Control point detection . . . . .	6
II-G	Statistics . . . . .	7
<b>III</b>	<b>Results</b>	7
III-A	Time-frequency coherence changes . . . . .	8
III-A.1	Sit-To-Stand . . . . .	8
III-A.2	Gait Initiation . . . . .	8
III-A.3	Sit-To-Walk . . . . .	8
III-B	Change-point analysis . . . . .	8
III-B.1	Sit-To-Stand . . . . .	8
III-B.2	Gait Initiation . . . . .	8
III-B.3	Sit-To-Walk . . . . .	9
III-B.4	Phase comparisons . . . . .	11
III-C	Weighting function . . . . .	11
<b>IV</b>	<b>Discussion</b>	11
<b>V</b>	<b>Conclusion</b>	13
	<b>References</b>	14
<b>VI</b>	<b>Appendix</b>	15
VI-A	Head angles . . . . .	15
VI-B	Change point detection with coherence slope . . . . .	16
VI-C	Applying weighting function to the transition phase . . . . .	16

**Abstract**—Predictive simulation is a powerful tool that can be used to examine the impacts of aging on complex movement behaviors. These models rely on neuromuscular controllers that modulate sensory feedback, including vestibular feedback, in order to transition between different movement phases. Current models, however, define the phase transitions based on the kinematics of movement without consideration for the underlying neurophysiological feedback mechanisms driving actual behavior. Here, we studied sit-to-walk movements, a challenging task commonly faced by aging populations, and examined how vestibular feedback is modulated for the control of balance. We estimated the coupling between an electrical vestibular stimulus and ground reaction forces in healthy participants (N = 16) while they performed a sit-to-walk task. Because sit-to-walk transitions are thought to be comprised of simultaneous transitions of standing up and walking, we also compared the sit-to-walk (STW) task to sit-to-stand (STS) (N = 8) and gait-initiation (GI) tasks (N = 8). Four main phases of vestibular control were identified for STW: quiet sitting, flexion, transition, and gait. Similarly, four main phases were identified for STS, though they differed after the first two: quiet sitting, flexion, rising/stabilizing, and quiet standing. In contrast, five main phases were identified for GI: quiet standing, adjustment I, adjustment II, transition, and gait. Importantly, the timings of the identified phases differed from the timings of the events used to define kinematic phases, and the magnitude of the vestibular responses was modulated gradually between phases. We also found that the vestibular modulation observed in STW could be explained as a sharp shift from an STS task just after flexion, around seat-off, into a GI task starting at transition. These results demonstrate that defining the timing of neuromuscular controllers in predictive simulation based on neurophysiological events may be better suited to improving their accuracy.

## I. INTRODUCTION

Advances in healthcare have led to increased life expectancy, causing a rise in the elderly population. With this aging global population, there is an escalating demand for care [1]. To prevent the demand from surpassing the capacity of caregiving services it is important to promote independent living for elderly individuals as long as possible. Therefore, there is an increasing need to examine the impacts of aging. Standing up from a seated position is one of the fundamental tasks of daily life, executed an average of 60 times a day [2]. Failure to perform this task is one of the key indicators that a person requires additional assistance with daily life. Rising from a chair is a challenging balance task as the center of mass (CoM) needs to move over the center of pressure (CoP) which compromises stability, in order to gain sufficient momentum to propel the body forward. As a result, falls are common during rising for the elderly, with difficulty in rising being a key risk factor for falls [3]. Many variables contribute to the increased difficulty with rising in aging populations such as a decline in sensory acuity, neuromuscular capacity, and cognitive function [4], [5]. As it remains difficult to isolate these variables in experimental studies, neuromusculoskeletal models are useful. To explore the interconnectivity of these variables we need models that predict movements [6]. To do that the simulations require a neuromuscular controller that can modulate sensory feedback between predefined phases.

Activation patterns of muscles engaged in balance control are influenced by sensory inputs including the vestibular sensory input. The vestibular system detects movements of the head in space and sends descending control signals to maintain stability. Predictive simulation models usually imitate proprioceptive and vestibular feedback to control the activation of the muscles. A proportional derivative control signal that acts on the trunk's orientation can be used in the model to replace natural vestibular feedback. The feedback gains within these models, however, are either constant or modulated according to kinematic phases [7], [8], [9], [10]. Kinematic phases are commonly defined based on kinematic events that can be identified through observable changes in force, accelerations, etc. They are however not rooted in the neurophysiology of feedback control and there is a lack of justification for using them in predictive simulation. In fact, when the timings of the change between controllers in predictive simulations are optimized to best resemble biological control, the resulting transition timings differ from the ones based on kinematic phases [6].

Vestibular feedback gains change throughout movements [11], [12]. During quiet standing, for example, variations on whole-body sway that are disruptive to balance stability are compensated by appropriately generated muscular torques modulated by vestibular feedback. On the other hand, to initiate gait, whole-body movements larger than normal balance sway are needed to move the center of mass over the base of support to accelerate the body. If vestibular feedback gains remained at levels maintained during standing balance, vestibular-driven feedback signals would impede the intended whole-body acceleration. Therefore the vestibular feedback gains need to be downregulated before the initiation of movement to enable a change of sensorimotor state. This has been shown by monitoring the influence of the vestibular system on human balance control in vivo by quantifying the magnitude of vestibular-evoked balance responses using electric vestibular stimulation (EVS) [12]. Prior to the onset of movement, there is an interruption of the vestibular balance stabilizing mechanisms that only return once the transition to gait has been achieved. These results suggest that the brain maintains separate control policies for quiet standing and locomotion, and must disengage one to transition to the other. They also align with the theory of optimal feedback control, a prominent motor control theory, which suggests that sensory feedback gains are optimized continuously according to the task. Specific postures and movements have a specific control policy that employs specific feedback gains. In order to engage a new control policy the previous one must be disengaged by changing the current feedback gains [13]. In other words, the different control policies can be attributed to different sensorimotor control phases within the movement.

In the current study, we aim to establish the contribution of vestibular feedback while standing up from a seated position, given the importance of this task in understanding balance control. Since the majority of standing up transitions are followed by walking among healthy individuals [14], we aim to assess a sit-to-walk (STW) task. As STW simultaneously

combines standing up and walking we extended our research aim to include a sit-to-stand (STS) and gait initiation (GI) task and assess any differences with STW. The aim of the current study is therefore to determine the vestibular control phases in STW compared to STS and GI. We hypothesized that several control phases could be extracted from the vestibular responses of each task and that the sensorimotor control phases of STW may be described by separate contributions from STS and GI tasks. Based on previous studies on vestibular responses during a GI task [12], 3-5 phases were expected in each task. Three tasks, STW, STS, and GI, were performed by healthy participants while being subjected to a vestibular disturbance. The coupling between the mediolateral ground reaction forces and the vestibular disturbance signal was calculated to quantify the vestibular evoked responses for each of the three conditions.

## II. METHODS

### A. Subjects

16 healthy subjects without any history of neurological or muscular disorders participated in the experiment. The study was approved by the TU Delft Human Research Ethics Committee. The experimental protocols were explained to each subject and written consent was obtained prior to participation in the experiment. The subject pool included 8 male and 8 female subjects, age  $24.8 \pm 1.5$  years, height  $1.74 \pm 0.09$ m, and weight  $71.2 \pm 13.7$ kg (*mean*  $\pm$  *SD*).

### B. Protocol

Three separate tasks were performed in the experiment to study how the modulation of vestibular feedback differs depending on the characteristics of the task. The tasks were: STW (initiating gait from a seated position), STS (standing up from a seated position), and GI (initiating gait from a standing position). Each task was repeated 80 times. All participants performed the STW task (16). Half of the participants also performed the STS task (8) while the other half performed the GI task (8). During the STW and STS tasks, the participants began the task in a seated position. The height of the seat was set to the approximate height of the participant's knee. After the height of the chair was fixed, the feet were brought closer to the chair such that the knee angle was  $75^\circ$  to facilitate standing up. The initial stance width was determined in all tasks based on the hip width. The initial position of the feet was marked with tape to ensure uniformity between trials. In the STW and GI tasks, participants were instructed to walk at approximately 0.5 m/s. Several practice trials were performed where the desired cadence of 60 steps/minute was controlled by a metronome. During the recorded trials the speed was tracked by the experimenter and verbal instructions were provided when needed. All tasks were performed with the head tilted back such that Reid's plane was oriented at  $18^\circ$  to maximize the vestibular evoked responses. A laser was secured to the participant's head and they were instructed to keep the laser at a target on a wall opposite them to ensure the correct head orientation. The experimenter visually monitored the

inclination angle of the head during the trial. Participants were instructed not to swing their arms or use them to push off their thighs while standing up, but arm movement remained otherwise unrestricted.

The participant began each trial in an initial position, quiet standing for GI and quiet sitting for STW and STS. Electrical vestibular stimulation (EVS) started 3 seconds after the start of the recording and lasted for 18 seconds. An audible cue was used to indicate when participants could start their movement. The audible cue was set to occur 9-11 seconds after the start of the recording. For the STW and GI tasks, the participants were instructed to walk, starting with the right leg, towards a wall located 3.5m away and remain standing there until the trial had ended. For the STS task, the participants were instructed to stand up at the audible cue and remain standing quietly until the trial had ended.

### C. Stimulus

During the trials, participants were subjected to EVS applied to the mastoid processes on each side delivered in a binaural bipolar configuration. EVS provides a craniocentric vestibular error signal by modulating the firing rate of the vestibular afferents without affecting other key balance-related sensory channels. When applied in a bilateral bipolar configuration with the head facing forward, the stimulus causes a sensation of rotation about an axis directed backward and slightly upwards (close to  $18^\circ$ ) relative to Reid's plane [15]. EVS primarily activates head roll responses, with relatively small linear responses from otolithic signals as the otolithic signals are nearly canceled due to the near symmetry of the afferent population [16], [17], [18], [19]. This virtual vestibular error signal significantly impacts balance during standing, leading to compensatory muscle and whole-body responses. These consistent whole-body responses can be used to examine the transformation of vestibular signals to balance control in humans.

A stochastic signal was designed for the stimulation with a bandwidth of 2.5-10.5Hz. The stimulus was generated by bandpass filtering a Gaussian white noise signal (3-order Butterworth) that was scaled to produce a peak amplitude of 4.5 mA (root mean square 0.85 mA). Each signal lasted 18 seconds providing enough time to perform any of the tasks. The signals were created using Matlab software (2020b version, MathWorks, Natick, MA, USA) and delivered with a stimulator (STMISOLA, Biopac, Goleta, CA, USA). The stimulator was connected through two wires to carbon rubber electrodes ( $9\text{cm}^2$ ) coated with conductive gel (Spectra 360, Parker Laboratories, Fairfield, NJ, USA) which were secured over the mastoid processes with adhesive tape.

### D. Instrumentation

The experiments were performed in the Department of Biomechanical Engineering at the Mechanical, Maritime, and Materials Engineering faculty at the Delft University of Technology. Ground reaction forces (GRF) and torques in three dimensions were recorded by five force plates (Kistler B.V., Eemnes, The Netherlands) at a frequency of

500 Hz. One force plate was fastened to an adjustable chair to record the GRF during sitting, Figure 1. The other four force plates formed a 1.7m measurable distance which was embedded in a walkway spanning 3.5m in total. When seated, the participant's feet rested on the first two force plates that made up the walkway. Whole-body kinematics were recorded with a 14-camera motion capture system (Qualisys, Göteborg, Sweden) at a frame rate of 100 Hz. 55 reflective markers (including 6 clusters) were attached to the following anatomical landmarks: head of the first and fifth metatarsal, head of the second distal phalanx, medial and lateral malleolus, calcaneus, rigid cluster on the lower leg, tibial tuberosity, fibular head, medial and lateral femoral epicondyle, rigid cluster on the upper leg, greater trochanter, anterior iliac spine, posterior iliac spine, first thoracic vertebrae, acromion process, rigid cluster on the upper arm, lateral humeral epicondyle, ulnar styloid, and 4 additional markers were placed on the front, back, right side and left side of the head. A trigger signal was used to initiate the start of the motion capture system recording and was recorded on a separate DAQ (NI USB-6001, National Instruments, Austin, TX, USA) together with the electrical stimulation for synchronization of the two recordings. A custom-made recording software was written in Labview (2018 version; National Instruments, Austin, TX, USA).

#### E. Analysis

All data analysis was performed using Matlab (2020b version, MathWorks, Natick, MA, USA). The onset of movement was identified for all tasks as the first instance that the absolute value of the anteroposterior force was greater than 4 standard deviations from the baseline. Baseline was defined as the first 5 seconds of the recording of the force plate on the chair, for the GI task the baseline was defined as the first 5 seconds of the recording of the force plate under the right foot. The recordings were normalized to the average time between two events across all trials of all subjects. For STW and GI, we used the time between the onset of movement and the third toe-off to normalize the data. For STS, we used the time between the onset of movement and the time point when the participants were fully upright. Toe-offs were identified as the last instant when the anteroposterior speed of the marker on the head of the second distal phalanx on each foot was below one standard deviation away from its mean value during quiet sitting. The time point that participants were fully upright was identified as the time when the marker on the first thoracic vertebrae had reached 95% of its maximum height.

A few additional kinematic events were defined to better characterize the behaviors within the task at various points in time. These events included: the seat-off (when the vertical force component of the seat force plate dropped below 5% of the body weight), and heel-strikes (the last instant when the height of the marker on the calcaneus of each foot was above 10% of its peak height).

The relationship between the summed GRF of all five force plates, and the EVS signal was estimated using time-

frequency coherence based on continuous Morlet wavelet decomposition [20]. This method has been used in previous studies to estimate the changes in vestibular-evoked responses [11], [12], [20], [21]. When the head faces forward, the perturbation resulting from the EVS is directed medio-laterally, therefore the mediolateral shear forces were used in the analysis. Coherence as well as gain and auto spectra of the output were estimated using the following equations:

$$Coherence = \frac{|S_{xy}|^2}{S_{xx}S_{yy}} \quad (1)$$

$$Gain = \frac{|S_{xy}|}{|S_{xx}|} \quad (2)$$

$$Autospectra = S_{yy} \quad (3)$$

In equations 1-3  $S_{xy}$  is the time-dependent cross-spectrum between the EVS and the shear force of interest.  $S_{xx}$  and  $S_{yy}$  are the time-dependent auto-spectra of the EVS (input) and the mediolateral shear forces (output) respectively.

Average coherence was calculated as the average coherence across the stimulated frequencies (2.5-10.5Hz).

#### F. Control point detection

Two additional analyses were used to objectively identify changes in vestibular sensorimotor control within a task and between tasks based on the variations in coherence and in that way define sensorimotor control phases within the tasks. First, to identify points at which the coherence level changed significantly during each task, a change point analysis was performed on the coherence level of each task, averaged over all participants. The change point analysis detects statistically significant changes in the mean by separating the data set into several regions that minimize the sum of the residual error of each region from its local mean. In that way, it is an objective way to estimate changes in vestibular responses, independent of kinematic phases, based only on vestibular feedback. This approach identifies significant changes in the mean coherence and therefore assumes an explicit shift from one control state to another. Since significant changes in coherence have been linked to explicit changes in control states during gait initiation [12], this method is expected to be sufficient to identify distinct control phases in the observed tasks. Since 3-5 phases were expected for each task, a maximum of 5 change points was used to extract the main phases. Since movements involved in switching between phases are subjected to various sensorimotor delays [22], [23], a minimum of 200ms between the change points was used.

Second, in order to describe the STW task in terms of STS and GI, a weighted model combining STS and GI was used and compared to the actual STW results. The weighting functions represent how much of STW behavior can be attributed to STS ( $\omega_s$ ) or GI ( $\omega_g$ ). The weighting functions  $\omega_s$  and  $\omega_g$  were computed as a cumulative (normal) distribution function and reversed cumulative (normal) distribution function, respectively, where  $\omega_s = 1 - \omega_g$ . The

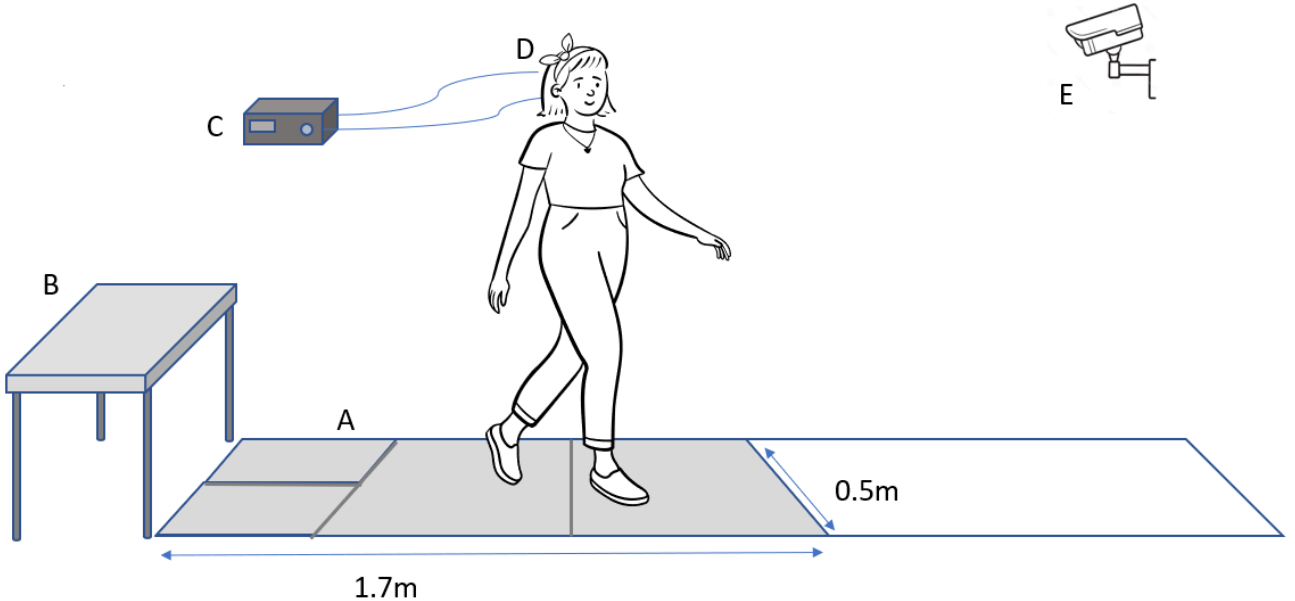


Fig. 1: A sketch of the setup of the experiment showing A: the four force plates on the floor which made up a 1.7m measurable walkway, B: The adjustable chair with one force plate, C: the stimulator, D: wires connected to electrodes secured to the mastoid processes, E: motion capture camera

optimal values of  $\mu$  (the switching time point) and  $\sigma$  (the dispersion of the function) of the functions were determined by minimizing the error when comparing the function's output to the observed STW data. These parameters indicate when STW behavior transitions (i.e.,  $\mu$ ) from an STS task into a GI, or more specifically a locomotion task, and how gradual the switch between the two tasks occurs (i.e.,  $\sigma$ ). The average coherence of STS and GI were multiplied with their respective weighting functions  $\omega_s$  and  $\omega_g$  and then summed together to predict the average coherence in the STW task. To correctly align the three tasks, the average coherence during GI was shifted by 0.32s, that way the third toe-offs of STW and GI were aligned in time.

### G. Statistics

Average coherence was used to determine whether the three tasks were significantly different at each phase determined by the change point analysis. A linear mixed model with the condition as the fixed factor and subject number as the random factor was performed to examine the main effect of condition (i.e., STW, STS, and GI) on average coherence. Where main effects were observed, pairwise comparisons with Bonferroni corrections were used to examine differences between separate conditions. The tests were performed in SPSS (26 version, IBM, Armonk, NY, USA).

## III. RESULTS

16 participants successfully performed 80 trials of STW, as well as 80 trials of either STS or GI. Participant details can be seen in Table I. The participants performed the instructed task; walking 3.5m at a speed of approximately 0.5m/s (STW and GI), or standing up (STS), from their

TABLE I: Summary of participant characteristics for each task

	Nr of participants	Age (years)	Height (cm)	Weight (kg)	Excluded participants
STW	16	24.8	174.7	72.6	1
STS	8	24.6	174.1	72.1	0
GI	8	24.9	175.3	73.1	0

initial position; sitting (STW and STS) or standing (GI), while being subjected to vestibular stimulation. The average measured walking speed was  $0.51 \pm 0.07m/s$  in the STW task and  $0.47 \pm 0.04m/s$  in the GI task. During all tasks, the pitch angle of the participants' heads was tracked throughout the trials. It remained relatively stable throughout deviating on average  $0.21 \pm 1.28^\circ$ ,  $0.16 \pm 0.78^\circ$ , and  $0.40 \pm 1.12^\circ$  from the target angle for STW, STS and GI respectively. The biggest deviations in head pitch angle (up to  $10^\circ$ ) were seen around the time of seat-off during STW and STS. The effect of these deviations is that the vestibular evoked responses are  $\cos(10^\circ) = 98\%$  of what they would be with the correct head orientation. Due to the minuscule effect, the deviations were therefore deemed acceptable. One participant in the STW task was, however, excluded from further analyses since we observed deviations of up to 30 degrees in all 80 trials. The participant in question additionally performed 80 trials of GI where the head orientation was considered to be within an acceptable range. The subject was therefore not excluded from the GI analysis aside from the within-subject comparisons. No trials were excluded from the STS or GI analysis based on head orientation

### A. Time-frequency coherence changes

For each task, the time-frequency coherence was calculated for each participant. The results averaged over all participants can be seen in Figures 2, 3 and 4. The average coherence was additionally calculated for each task, Figure 5.

1) *Sit-To-Stand*: At the beginning of STS, the coherence was constant, being the strongest at approximately 3-7Hz, Figure 2. During this period the participants demonstrated small variations in sway and ground reaction forces (root-mean-square of  $0.23 \pm 0.02N$  for STW and STS respectively) through the force plates on the chair and under the feet. The first large deviations in force data can be seen when the torso is moved forward, shifting the center of mass to prepare for standing, marking the beginning of the movement. At the initiation of movement, as indicated by the anteroposterior force data, the coherence level had already dropped below what it was at the beginning of the task and remained low until around 1 second after the initiation or around the time of seat-off. At this time, the weight is shifted entirely to the feet and in the moments that follow the body is extended. With a smaller base of support and increased height of the center of mass, the stability is reduced. During this period the coherence increased again reflecting the increased balance demand. After the body had been fully extended there was a period where the coherence dropped slightly again, particularly at the higher frequencies 6-7Hz before it reached a constant level.

2) *Gait Initiation*: At the beginning of the GI task, the coherence was constant coherence at frequencies 3-7Hz, Figure 3. During this period the participants demonstrated small variations in sway and ground reaction forces (root-mean-square of  $0.25 \pm 0.03N$ ) through the force plates under the feet. Before the force data showed that the initiation of movement had begun the coherence started decreasing. Before gait begins, the swing foot is unloaded, during this period there was again an increased coherence which lasted until just after the first toe-off. After that coherence settled into a rhythm of high coherence during single support and low coherence during double support.

3) *Sit-To-Walk* : The STW task shows a strong resemblance to both STS and GI behavior. The beginning of the task shows a constant level of coherence at approximately 3-7Hz, Figure 4. During this period the participants demonstrated small variations in sway and ground reaction forces (root-mean-square of  $0.25 \pm 0.02N$ ) through the force plates on the chair and under the feet. The first large deviations in force data can be seen when the torso is moved forward, marking the beginning of the movement. Just as in STS, at the initiation of movement, the coherence level had already dropped below what it was at the beginning of the task and remained low until around 1 second after the initiation or around the time of seat-off. Following the seat-off the coherence increased again reflecting the increased balance demand. Thereafter the participant started walking, during this period there was a repeated rhythm of high coherence

during the single support and low coherence during double support of gait, just like in GI.

Figure 5 shows a within-subject comparison between STW, and STS and GI, showing the similarities between the tasks. It shows that the STW task closely follows the behavior of the STS task up until around  $t=1s$ , after that it closely follows the behavior of the GI task.

### B. Change-point analysis

The average time-frequency coherence was then used to separate the tasks into several phases using change point analysis, Figure 6.

1) *Sit-To-Stand*: A total of 4 phases were extracted by detecting changes in the mean coherence. They were defined as: quiet sitting, flexion, rising and stabilizing, and quiet standing.

During the quiet sitting phase, the coherence remained relatively constant, averaging  $0.07 \pm 0.04$ , Figure 6. The flexion phase started on average  $0.21s$  before the initiation of movement and lasted until just after the time of seat-off. During this phase, the coherence dropped significantly to  $0.05 \pm 0.02$ . However, out of the 8 participants, only 4 showed a clear suppression of the vestibular responses (the first change point being before the initiation). We will hereafter refer to those participants as responders and the rest as non-responders. The suppression of these 4 responders occurred on average  $0.20 \pm 0.21s$  prior to initiation of movement. The 4 responders additionally showed a significantly higher coherence level during quiet sitting,  $0.11 \pm 0.04$ , as opposed to  $0.04 \pm 0.02$  for the non-responders ( $p = 0.016$ ,  $t$ -statistic = 3.32). The next phase, rising/stabilizing, started around the time of seat-off and ended when the coherence had reached a constant level. This phase therefore encompasses the peak in coherence that occurs while rising and the slight drop in coherence that occurs following the rising, averaging  $0.19 \pm 0.03$ . Following the end of the movement, during quiet standing, when ground reaction forces had plateaued, the coherence remained relatively constant at around  $0.26 \pm 0.05$ .

2) *Gait Initiation*: A total of 5 phases were extracted by detecting changes in the mean coherence. They were defined as: quiet standing, adjustment I, adjustment II, transition, and gait.

During the quiet standing phase, the coherence remained relatively constant, averaging  $0.17 \pm 0.06$ , Figure 6. The quiet standing phase ended on average  $0.57s$  before the initiation of movement. The subsequent phase, the adjustment phase, is split into two phases, adjustment I, where the coherence starts dropping, and adjustment II, where the coherence drops slightly further reaching a minimum around the time of kinematic initiation and then starts increasing again. Out of the 8 participants, 7 showed a clear suppression of the vestibular responses (first change point being before the initiation). During adjustment I the coherence decreased, averaging  $0.12 \pm 0.06$  during the phase. During the adjustment II phase, the coherence dropped to a level of  $0.09 \pm 0.06$ . During the transition period, the coherence returned reaching  $0.15 \pm 0.09$ . Following the first toe-off, at the start of gait,

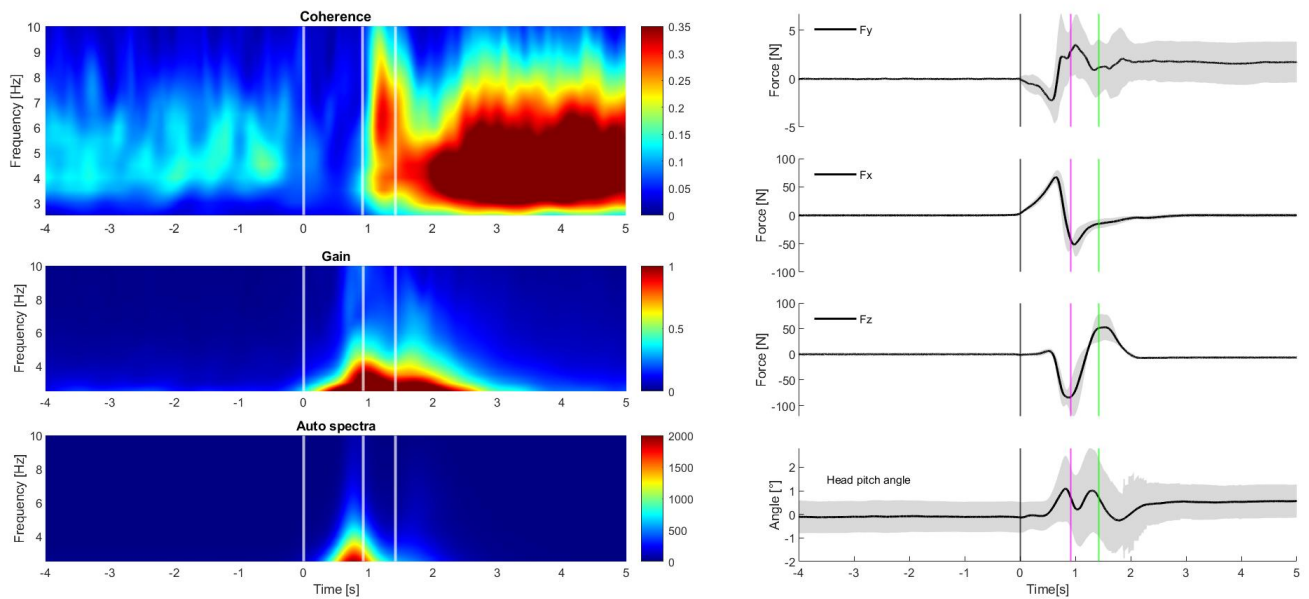


**Fig. 2:** Left: Averaged time-frequency coherence, gain, and autospectra results for the STS task across all subjects. Right:  $F_y$  (mediolateral),  $F_x$  (anteroposterior), and  $F_z$  (vertical) forces of all 5 force plates summed, as well as the angle that the head made with respect to the target head orientation. Shaded areas represent 1 standard deviation from the mean. The vertical lines show kinematic events: black is movement initiation, pink is the seat-off and green is the time when participants were fully upright (all white in the figures on the left). Time was normalized based on the duration between initiation and the time point when participants were fully upright

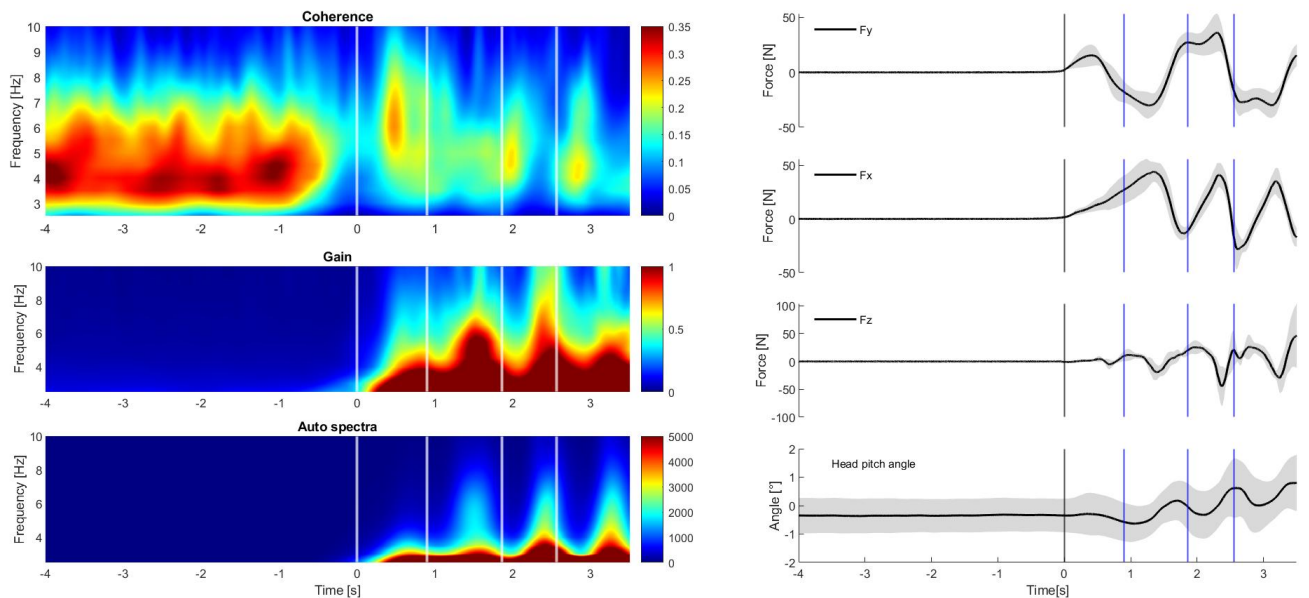


**Fig. 3:** Left: Averaged time-frequency coherence, gain, and autospectra results for the GI task across all subjects. Right:  $F_y$  (mediolateral),  $F_x$  (anteroposterior), and  $F_z$  (vertical) forces of all 5 force plates summed, as well as the angle that the head made with respect to the target head orientation. Shaded areas represent 1 standard deviation from the mean. The vertical lines show kinematic events: black is movement initiation and the blue lines show the first, second, and third toe-off (all white in the figures on the left). Time was normalized based on the duration between initiation and the third toe-off.

the coherence settled into a rhythm of high coherence during single support  $0.11 \pm 0.07$  and low coherence during double support  $0.08 \pm 0.04$ .

3) *Sit-To-Walk*: A total of 4 phases were extracted by detecting changes in the mean coherence. They were defined as: quiet sitting, flexion, transition, and gait. During the quiet

sitting phase, the coherence remained relatively constant averaging  $0.09 \pm 0.05$ , Figure 6. The flexion phase started just before the initiation of movement, on average  $0.27s$  before the kinematic initiation, during this phase the average coherence dropped to  $0.05 \pm 0.02$ . However, out of the 15 participants, only 7 showed a clear suppression of the

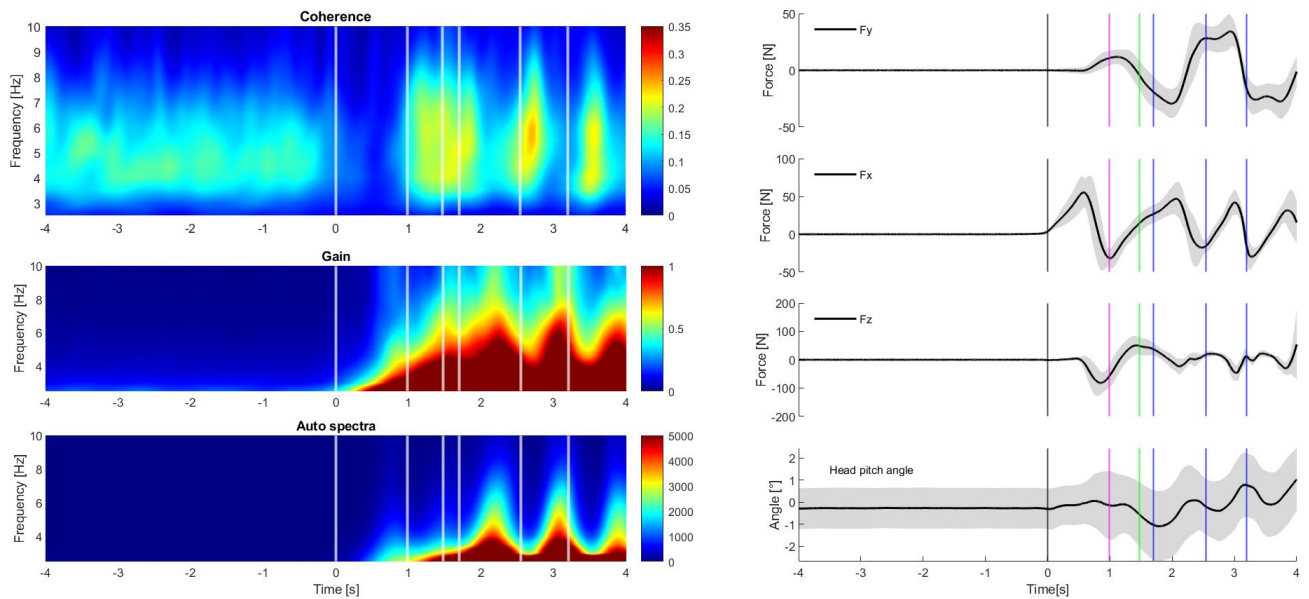


**Fig. 4:** Left: Averaged time-frequency coherence, gain, and autospectra results for the STW task across all subjects. Right:  $F_y$  (mediolateral),  $F_x$  (anteroposterior), and  $F_z$  (vertical) forces of all 5 force plates summed, as well as the angle that the head made with respect to the target head orientation. Shaded areas represent 1 standard deviation from the mean. The vertical lines show kinematic events: black is movement initiation, pink is seat-off, green is the time when participants were fully upright, and the blue lines show the first, second, and third toe-off (all white in the figures on the left). Time was normalized based on the duration between initiation and the third toe-off.

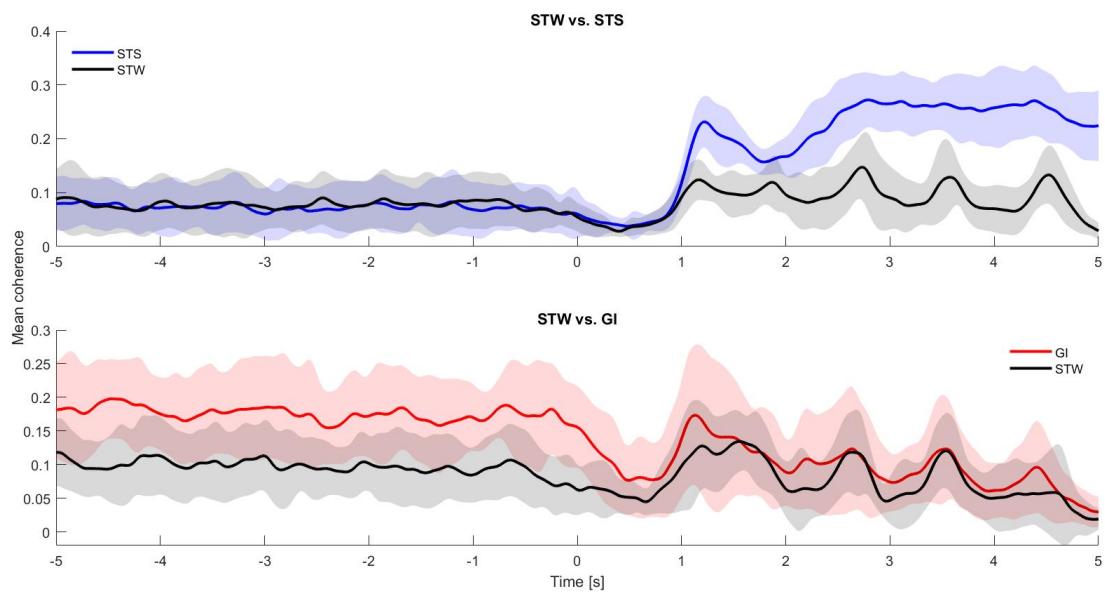


**Fig. 5:** Within-subject comparison of STW and STS (top) and STW and GI (bottom). Average coherence is plotted, the shaded areas represent 1 standard deviation from the mean. The apparent difference between STW results between the groups is due to between-subject variability and is not significant. GI results have been shifted in time to align the timings of the third toe-off of GI and STW

vestibular responses before the initiation (first change point before the initiation), among these 7 responders the suppression occurred on average  $0.30 \pm 0.16s$  (timing of first change point). Interestingly, out of these 7, the 4 responders that had performed STS had additionally showed a suppression of the vestibular responses in that task as well. The responders here also showed a significantly higher coherence level during

quiet sitting,  $0.12 \pm 0.04$ , as opposed to  $0.05 \pm 0.03$  for the non-responders ( $p=0.003$ ,  $t$ -statistic=3.67). The coherence returned just after the time of the seat-off, at the start of the transition phase, and reached a height of  $0.13 \pm 0.07$ . Following the first toe-off, start of gait, the coherence dropped once again and settled into a rhythm of high coherence during single support  $0.13 \pm 0.05$  and low coherence during the

double support phases of gait  $0.09 \pm 0.05$ .

4) *Phase comparisons*: STW has the same first two phases as STS: quiet sitting and flexion, although the flexion phase starts slightly earlier in STW, Figure 6. During the third phase, the tasks diverged from each other. The transition point between phases 2 and 3, flexion and transition, and flexion and rising/stabilizing in STW and STS respectively, occurred at 1.01s after the initiation of movement, in both tasks. Following the end of the transition phase of STW, just after the first toe-off, the gait started, during this phase the behavior is similar to the gait of the GI task. The alignment of the STW and GI tasks is based on the timing of the third toe-off. In STW, the timing between the change point, which determines the beginning of the transition phase, and the third toe-off is 2.19s. In the case of GI, the timing between the change point that determines the beginning of the transition phase and the third toe-off is 2.25s. Additionally, the transition phase is slightly longer in STW, lasting 0.91s, while in GI it only lasts 0.68s.

A statistical comparison of the coherence level of each phase between the tasks, Table II shows that there was not a significant difference between STW and STS during quiet sitting or flexion but the two tasks were significantly different during the third phase, transition and rising/stabilizing respectively. Comparing STW and GI shows that the two tasks were significantly different until the second-to-last phase, the transition, after that the STW and GI followed the same behavior.

### C. Weighting function

A cumulative distribution weighting function was applied to STS and GI to make a model of the expected STW behavior and compared to the observed behavior of STW, Figure 7. The error between the model and STW was minimized when  $\mu = 1.06$  and  $\sigma = 0$ . The model closely resembled the observed behavior of STW, being identical to STS until  $t = 1.06s$  and to GI after that.

## IV. DISCUSSION

The main finding of this study is that the vestibular influence on balance control during a sit-to-walk task undergoes three transitions between four distinct sensorimotor control phases. The first two phases are similar to those observed in a sit-to-stand task, where an initially seated participant flexes forward to initiate standing. The latter two phases closely match the transition to walking observed during gait initiation, where the coherence rises for an extended period and then falls into a rhythm synchronized with the gait cycle. The transition point between STS and GI occurs approximately around the time of seat-off. In all three conditions, a suppression of the vestibular responses is needed to initiate movement from a motionless position as it involves disengaging one control policy before implementing another one.

Although some of the sensorimotor control phases that emerged from the change point analysis appear similar to the ones that are commonly used to define kinematic phases

[24], [25], [26] there are crucial differences between them. In all three tasks, the first change point, which marks the switch between the first and second phases (quiet sitting and flexion for STW and STS, and quiet standing and adjustment I for GI) comes before the kinematic event which marks the initiation of movement. That is, the sensorimotor control phase flexion starts earlier than the corresponding kinematic phase due to the suppression of vestibular responses that enables the initiation of movement. The kinematic event that commonly marks the end of the flexion phase, the seat-off, on the other hand, is remarkably close to the second change point which marks the switch in control phases from flexion to the transition phase or the rising/stabilizing phase for STW and STS, differing by only 0.03s and 0.09s, respectively. The switch in GI control phases between adjustment II and transition does not correspond to any observable kinematic event. It occurs 2.25s before the third toe-off which is comparable to STW as the second change point of STW occurred 2.19s before the third toe-off. In both STW and GI, the transition phase encompasses the first toe-off. As both the transition and the first swing phase are characterized by high coherence, the vestibular responses show no distinction between them and they appear as one phase. It is possible that the apparent merging of these two phases occurs because the unloading of the swing foot starts already during the transition phase.

In STS, the kinematic phases that commonly follow the flexion are momentum transfer, extension, and stabilization. In terms of vestibular feedback, the last three kinematic phases appear to be combined in one sensorimotor control phase, the rising/stabilization phase. This phase however is long, roughly 1.4s, and encompasses multiple changes in the coherence level, Figure 6. The phase starts closely following the seat-off, in the beginning, the coherence rises rapidly before it reaches a peak and starts decreasing again, towards the end of the phase the coherence has started increasing once again. The drop in coherence level that occurs in this phase could be explained by the muscle activation patterns during the movement. During the stabilization that follows standing up, the muscle activation of lower leg muscles is momentarily reduced before the co-contraction associated with quiet standing begins [27], [28].

Like in kinematic phases, subsequent gait during STW and GI can be separated into single support and double support phases with coherence being high during single support but low during double support. This trend is in line with what would be expected due to stabilizing demands being higher during single support than double support, and similar results have been observed in previous work [29]. Tisserand et al. (2018) reported the opposite result of high coherence during double support of gait but low during single support [12]. The difference can likely be attributed to different walking speeds, ours was constrained at 0.5 m/s while it was unrestricted for Tisserand et al. (2018). Walking speed is known to affect the timing of the peak coherence during gait with higher speed pushing the peak earlier into the stance phase [21].

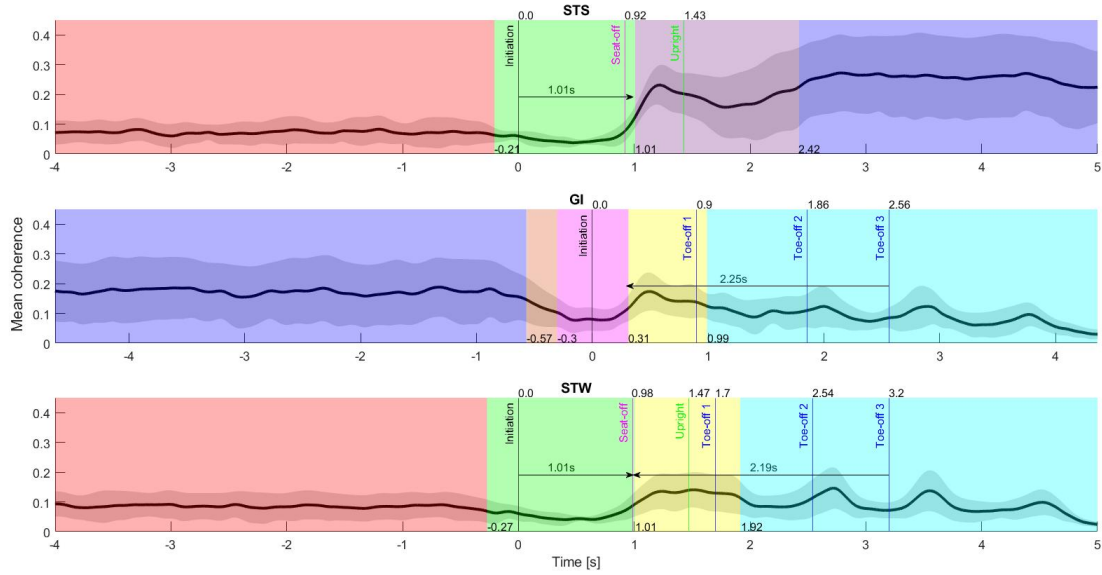


**Fig. 6:** Results from the change point analysis of STS (top), GI (middle), and STW (bottom). Average coherence is plotted, the shaded areas represent 1 standard deviation from the mean. The change points are used to separate the three tasks into phases. Colored areas depict the phases of each task as determined by the change points, red: quiet sitting, green: flexion, purple: rising/stabilizing, blue: quiet standing, orange: adjustment I, pink: adjustment II, yellow: transition, cyan: gait. The exact timings of the change points can be seen at the bottom of the graphs. Vertical lines show kinematic events, black: initiation of movement, pink: seat-off, green: participant is fully upright, blue: toe-offs. The exact timings of the kinematic events can be seen on top of the graphs. Note that the GI task is shifted in time to align the third toe-off of STW and GI together

**TABLE II:** Statistical comparison of mean coherence of each phase between the tasks. Phases are defined from the change point analysis, Phase 1: quiet sitting/quiet standing, phase 2: flexion/adjustment (I and II), and phase 3: rising-stabilizing/transition

	F	Main effect	STW vs STS	STW vs. GI	STS vs GI
Phase 1	11.030	0.001	1	0.001	0.002
Phase 2	6.413	0.009	1	0.007	0.039
Phase 3	4.346	0.031	0.030	1	0.386

In general, the level of coherence reflects the relative contribution of vestibular feedback to the ongoing motor output, which in turn is thought to relate to the stabilization demands of balance control at any given moment. For example, the magnitude of the coherence is higher during standing than sitting as the center of mass is much higher and over a smaller base of support. In all three tasks, the coherence dropped before the initiation of movement indicating that a suppression of vestibular responses is needed to overcome the balance-correcting responses that are engaged during quiet sitting and standing. Without the suppression, initiation of movement would be impeded since the intended movement to lean forward and "fall" into the next phase would be limited by balance correcting mechanisms from the previous control policy. Our results suggest that the timing of the suppression depends on the magnitude of the coherence prior to the suppression; during tasks with high vestibular feedback, such as standing, coherence decreases earlier relative to the initiation of movement as compared to sitting tasks with low vestibular feedback. A similar mechanism may also explain the difference between the responders and non-responders during STW and STS conditions. For participants with a high

sensitivity to the electrical stimulus (i.e., high coherence), transition points from quiet sitting to flexion phases were identified prior to the onset of motion. On the other hand, for participants with low sensitivity to the electrical stimulus, the coherence level is seemingly already low enough in order to initiate movement from the current position.

Knowing the change in magnitude of vestibular feedback at any given time in the tasks in question is valuable for predictive simulation as the feedback gains can be adjusted throughout the movement. In current models, the feedback gains are determined by the controller which is specified for each kinematic phase, and kinematic events facilitate the switch between the kinematic phases. The problem with using kinematic phases to determine the magnitude of vestibular feedback however is that they are identified based on changes in measurable parameters such as force and velocity and their purpose is to simplify kinematic analysis and lend understanding of the progression of each phase, they are not rooted in neural control. Adapting the modulation of vestibular feedback gains in predictive simulation to match the measured feedback gains observed here may therefore improve their accuracy. Our results are limited because the

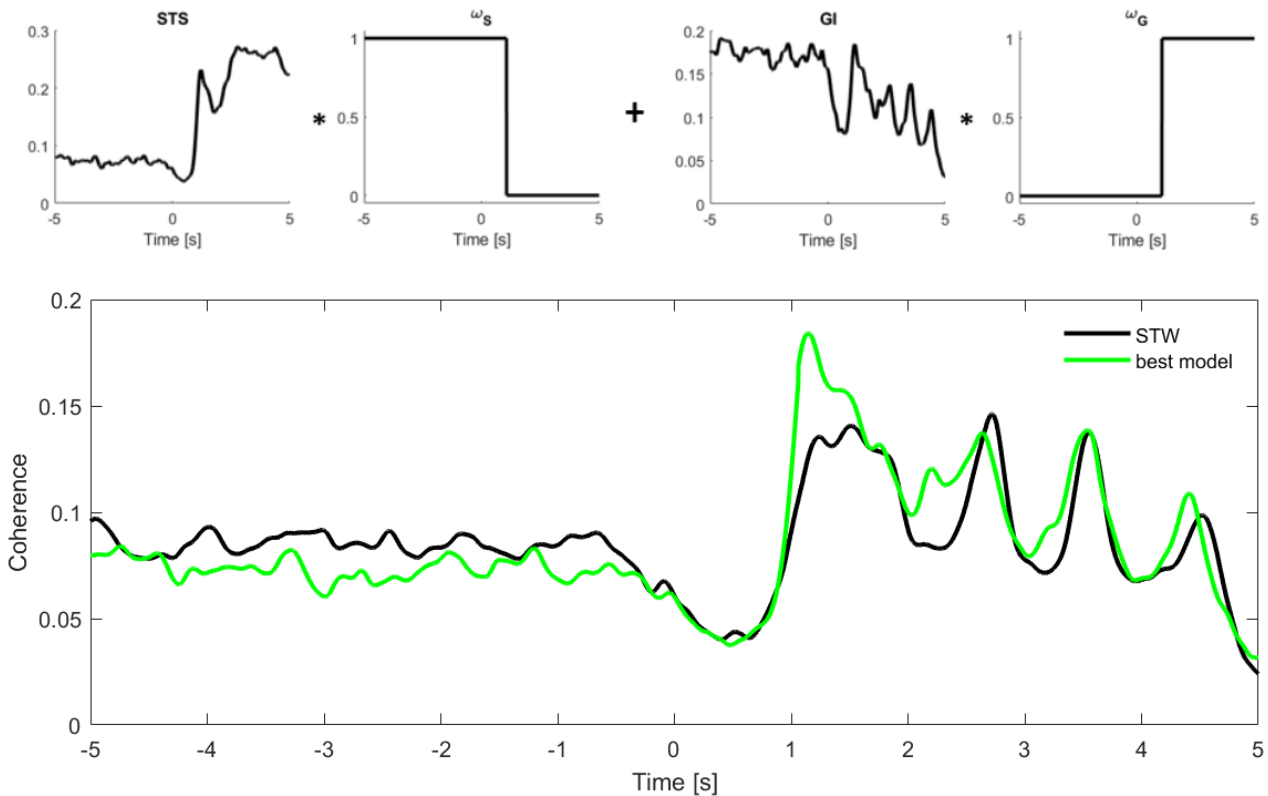


Fig. 7: Top: Components of the weighted model, average coherence during STS and GI multiplied by a weighting function (and the inverse) with  $\mu = 1.06$  and  $\sigma = 0$  which provided the optimal model. Bottom: The resulting model of STW behavior compared to the observed STW behavior

change point analysis assumes an explicit shift from one control policy to another. However, the results show that the change in coherence is never abrupt, it adapts gradually between phases. Although our current results do not offer insight into the gradual adaptation of vestibular responses, it is possible that these gradual changes may also be due to additional factors such as delays caused by muscle activation, neural processing and nerve conduction. Using the slope of the coherence rather than the mean to identify change points could be helpful in that regard as it better captures the properties of the change, fig 11 or another approximation method such as Taut-string [30] could be useful in future studies. Another assumption that is made in simulation is that the vestibular and proprioceptive feedback are regulated with the same transition points. This might not be the case. According to optimal feedback control theory, each sensory feedback loop is adjusted separately depending on the challenges of the task at hand by minimizing a task-dependent cost function [31].

Our study had a few additional limitations. Results of the head orientation show that there is a small drift in the positive pitch direction. This is a result of improper placement of the laser that controlled the head angle. This deviation was overall very small and is not expected to have affected the vestibular responses. Lastly, the results are limited by the limited number of participants, especially

considering that not all participants showed a preemptive response in the suppression of vestibular responses. The limited number of participants was unavoidable however since lab time was limited and participants' sensitivity to EVS was unpredictable. Additionally, seeing the difference in vestibular sensitivity between the subjects was an insightful addition.

## V. CONCLUSION

Four main sensorimotor control phases can be extracted from the vestibular responses of an STW task: quiet sitting, flexion, transition, and gait. The first two are similar to those observed during an STS task and the latter two are similar to those observed during GI. In terms of vestibular responses, STW can therefore be described as a discrete transition from STS to GI, with the shift occurring around the time of seat-off. The timings of the control phases differed from the timings of the events used to define kinematic phases. Therefore the use of kinematic phases to regulate neuromuscular controllers in predictive simulation should be reconsidered.

## REFERENCES

- [1] R. Wittenberg, L. Pickard, A. Comas Herrera, B. Davies, and R. Darton, "Demand for long-term care for older people in England to 2031," *Health Statistics Quarterly*, vol. 12, pp. 5–17, 2001.
- [2] P. M. Dall and A. Kerr, "Frequency of the sit to stand task: An observational study of free-living adults," *Appl Ergon*, vol. 41, no. 1, pp. 58–61, 2010. [Online]. Available: <https://www.ncbi.nlm.nih.gov/pubmed/19450792>
- [3] G. F. Fuller, "Falls in the elderly," *American family physician*, vol. 61, no. 7, p. 2159, 2000.
- [4] E. van der Kruk, A. K. Silverman, P. Reilly, and A. M. J. Bull, "Compensation due to age-related decline in sit-to-stand and sit-to-walk," *J Biomech*, vol. 122, p. 110411, 2021. [Online]. Available: <https://www.ncbi.nlm.nih.gov/pubmed/33915476>
- [5] E. Van Der Kruk, P. Strutton, L. J. Koizia, M. Fertleman, P. Reilly, and A. M. J. Bull, "Why do older adults stand-up differently to young adults?: investigation of compensatory movement strategies in sit-to-walk," *npj Aging*, vol. 8, no. 1, 2022. [Online]. Available: <https://dx.doi.org/10.1038/s41514-022-00094-x>
- [6] E. van der Kruk and T. Geijtenbeek, "A muscle-reflex controller to simulate age-related adaptation strategies in the sit-to-walk movement." XIX International Symposium on Computer Simulation in Biomechanics, 2023.
- [7] H. Geyer and H. Herr, "A muscle-reflex model that encodes principles of legged mechanics produces human walking dynamics and muscle activities," *IEEE Trans Neural Syst Rehabil Eng*, vol. 18, no. 3, pp. 263–73, 2010. [Online]. Available: <https://www.ncbi.nlm.nih.gov/pubmed/20378480>
- [8] D. Muñoz, C. De Marchis, L. Gizzi, and G. Severini, "Predictive simulation of sit-to-stand based on reflexive-controllers," *PLOS ONE*, vol. 17, no. 12, p. e0279300, 2022. [Online]. Available: <https://dx.doi.org/10.1371/journal.pone.0279300>
- [9] N. Waterval, K. Veerkamp, T. Geijtenbeek, J. Harlaar, F. Nollet, M. A. Brehm, and M. M. van der Krogt, "Validation of forward simulations to predict the effects of bilateral plantarflexor weakness on gait," *Gait Posture*, vol. 87, pp. 33–42, 2021. [Online]. Available: <https://www.ncbi.nlm.nih.gov/pubmed/33882437>
- [10] S. Song and H. Geyer, "A neural circuitry that emphasizes spinal feedback generates diverse behaviours of human locomotion," *The Journal of Physiology*, vol. 593, no. 16, pp. 3493–3511, 2015. [Online]. Available: <https://dx.doi.org/10.1113/jp270228>
- [11] C. J. Dakin, J. T. Inglis, R. Chua, and J. S. Blouin, "Muscle-specific modulation of vestibular reflexes with increased locomotor velocity and cadence," *J Neurophysiol*, vol. 110, no. 1, pp. 86–94, 2013. [Online]. Available: <https://www.ncbi.nlm.nih.gov/pubmed/23576695>
- [12] R. Tisserand, C. J. Dakin, M. H. Van Der Loos, E. A. Croft, T. J. Inglis, and J.-S. Blouin, "Down regulation of vestibular balance stabilizing mechanisms to enable transition between motor states," *eLife*, vol. 7, 2018. [Online]. Available: <https://dx.doi.org/10.7554/eLife.36123>
- [13] T. Cluff and S. H. Scott, "Online corrections are faster because movement initiation must disengage postural control," *Motor Control*, vol. 20, no. 2, pp. 162–70, 2016, cluff, Tyler Scott, Stephen H eng Comment 2015/04/29 Motor Control. 2016 Apr;20(2):162-70. doi: 10.1123/mc.2015-0027. Epub 2015 Apr 28. [Online]. Available: <https://www.ncbi.nlm.nih.gov/pubmed/25920075>
- [14] A. Kerr, Rafferty, Hollands, Barber, and Granat, "A technique to record the sedentary to walk movement during free living mobility: A comparison of healthy and stroke populations," *Gait and Posture*, vol. 52, pp. 233–236, 2017. [Online]. Available: <https://dx.doi.org/10.1016/j.gaitpost.2016.11.046>
- [15] R. C. Fitzpatrick and B. L. Day, "Probing the human vestibular system with galvanic stimulation," *Journal of Applied Physiology*, vol. 96, no. 6, p. 2301, 2004.
- [16] B. L. Day, "Vestibular-evoked postural responses in the absence of somatosensory information," *Brain*, vol. 125, no. 9, pp. 2081–2088, 2002. [Online]. Available: <https://dx.doi.org/10.1093/brain/awf212>
- [17] O. S. Mian, C. J. Dakin, J.-S. Blouin, R. C. Fitzpatrick, and B. L. Day, "Lack of otolith involvement in balance responses evoked by mastoid electrical stimulation," *The Journal of Physiology*, vol. 588, no. 22, pp. 4441–4451, 2010. [Online]. Available: <https://dx.doi.org/10.1113/jphysiol.2010.195222>
- [18] A. Tribukait and U. Rosenhall, "Directional sensitivity of the human macula utriculi based on morphological characteristics," *Audiology and Neurotology*, vol. 6, no. 2, pp. 98–107, 2001. [Online]. Available: <https://dx.doi.org/10.1159/000046815>
- [19] D. L. Wardman, J. L. Taylor, and R. C. Fitzpatrick, "Effects of galvanic vestibular stimulation on human posture and perception while standing," *The Journal of physiology*, vol. 551, no. 3, pp. 1033–1042, 2003.
- [20] J. S. Blouin, C. J. Dakin, K. van den Doel, R. Chua, B. J. McFadyen, and J. T. Inglis, "Extracting phase-dependent human vestibular reflexes during locomotion using both time and frequency correlation approaches," *J Appl Physiol (1985)*, vol. 111, no. 5, pp. 1484–90, 2011. [Online]. Available: <https://www.ncbi.nlm.nih.gov/pubmed/21868684>
- [21] P. A. Forbes, M. Vlutters, C. J. Dakin, H. van der Kooij, J. S. Blouin, and A. C. Schouten, "Rapid limb-specific modulation of vestibular contributions to ankle muscle activity during locomotion," *J Physiol*, vol. 595, no. 6, pp. 2175–2195, 2017. [Online]. Available: <https://www.ncbi.nlm.nih.gov/pubmed/28008621>
- [22] H. L. More and J. M. Donelan, "Scaling of sensorimotor delays in terrestrial mammals," *Proceedings of the Royal Society B: Biological Sciences*, vol. 285, no. 1885, p. 20180613, 2018. [Online]. Available: <https://dx.doi.org/10.1098/rspb.2018.0613>
- [23] M. Thangal, S. Naseel, and D. Maxwell, "Scaling of inertial delays in terrestrial mammals," *PLOS ONE*, vol. 15, no. 2, p. e0217188, 2020. [Online]. Available: <https://dx.doi.org/10.1371/journal.pone.0217188>
- [24] A. Kerr, D. Rafferty, K. M. Kerr, and B. Durward, "Timing phases of the sit-to-walk movement: Validity of a clinical test," *Gait posture*, vol. 26, pp. 11–6, 2007.
- [25] G. D. Jones, D. C. James, M. Thacker, and D. A. Green, "Parameters that remain consistent independent of pausing before gait-initiation during normal rise-to-walk behaviour delineated by sit-to-walk and sit-to-stand-and-walk," *PLoS One*, vol. 13, no. 10, p. e0205346, 2018. [Online]. Available: <https://www.ncbi.nlm.nih.gov/pubmed/30300414>
- [26] M. Schenkman, "Whole-body movements during rising to standing from sitting," *Physical Therapy*, vol. 70, no. 10, p. 638, 1990.
- [27] T. Nashrulloh, V. Biben, and F. A. Santi, "Pattern of muscle activation during sit to stand task in feet forward with 80° knee flexion using surface emg," *Proceedings of the 11th National Congress and the 18th Annual Scientific Meeting of Indonesian Physical Medicine and Rehabilitation Association*, pp. s 82–87, 2020.
- [28] W. Jeon, J. Whittall, L. Griffin, and K. Westlake, "Trunk kinematics and muscle activation patterns during stand-to-sit movement and the relationship with postural stability in aging," *Gait Posture*, vol. 86, pp. 292–298, 2021.
- [29] R. Magnani, S. Bruijn, J. van Dieën, and P. A. Forbes, "Stabilization demands of walking modulate the vestibular contributions to gait," *Scientific Reports*, vol. 11, no. 1, 2021. [Online]. Available: <http://hdl.handle.net/1765/136296>
- [30] L. Dumbgen and A. Kovac, "Extensions of smoothing via taut strings," *Electronic journal of statistics*, vol. 3, no. 2009, pp. 41–75, 2009.
- [31] J. Diedrichsen, R. Shadmehr, and R. B. Ivry, "The coordination of movement: optimal feedback control and beyond," *Trends in Cognitive Sciences*, vol. 14, no. 1, pp. 31–39, 2010. [Online]. Available: <https://dx.doi.org/10.1016/j.tics.2009.11.004>

## VI. APPENDIX

### A. Head angles

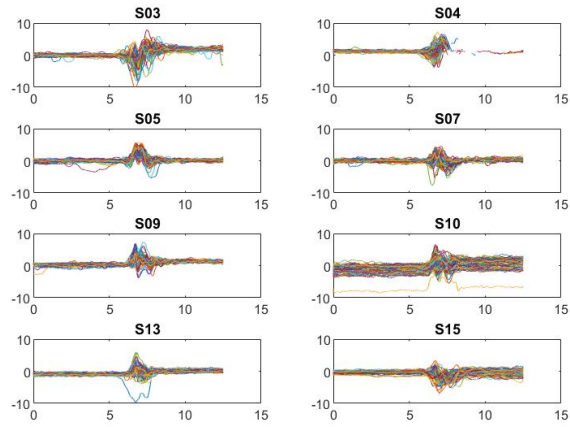


Fig. 8: Angle that the head made with respect to the target head orientation for the STS task, for each individual subject and trial

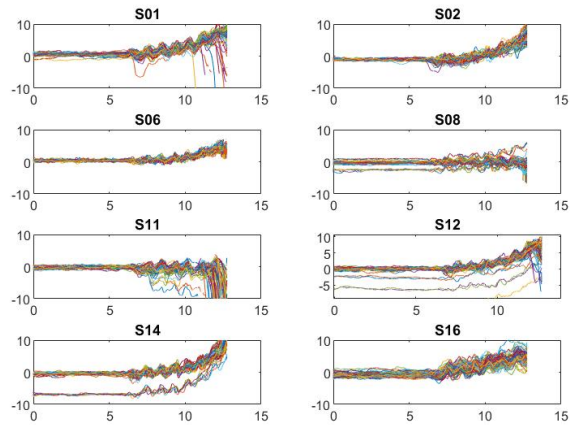


Fig. 9: Angle that the head made with respect to the target head orientation for the GI task, for each individual subject and trial

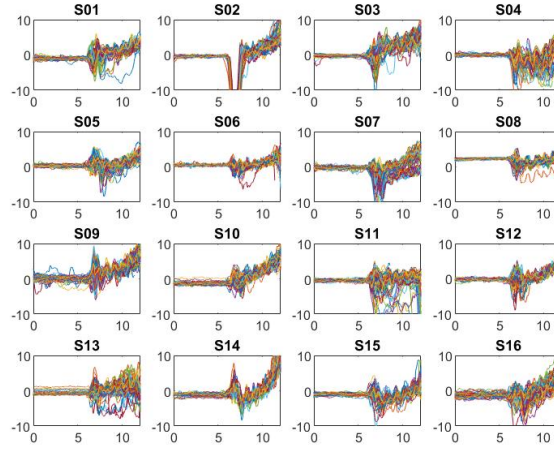


Fig. 10: Angle that the head made with respect to the target head orientation for the STW task, for each individual subject and trial

### B. Change point detection with coherence slope

In addition to the change point analysis that was done by detecting changes in the mean coherence, the change point analysis was performed by detecting changes in the slope of the coherence, Figure 11.

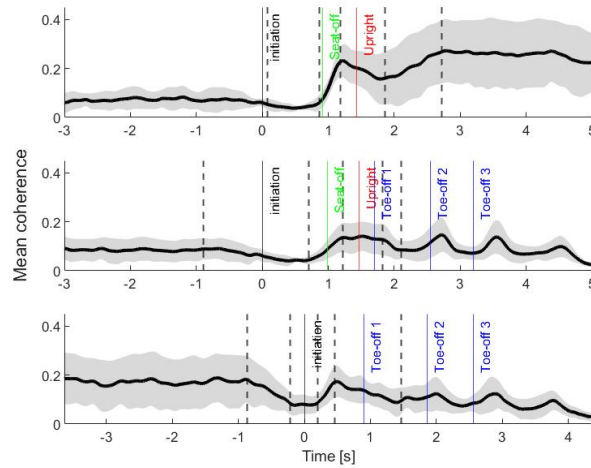


Fig. 11: Results from the change point analysis by detecting changes in the mean and slope, STS (top), STW (middle), GI (bottom). Average coherence is plotted, the shaded areas represent 1 standard deviation from the mean. Black dashed lines show change points colored lines show kinematic events. Note that the time axis is shifted for GI to align the third toe-off of STW and GI together

The change point analysis separated the STS task into 6 sections based on changes in the slope of the coherence. The slope coherence in the sections was 0.003 between points 1 and 2, 0.59 between points 2 and 3, -0.12 between points 3 and 4, and 0.14 between points 4 and 5. The GI task was also separated into 6 sections based on changes in the slope of the coherence. The slope coherence in the sections was -0.14 between points 1 and 2, 0.004 between points 2 and 3, 0.35 between points 3 and 4, and -0.08 between points 4 and 5. The STW task was also separated into 6 sections based on changes in the slope of the coherence. The slope coherence in the sections was -0.04 between points 1 and 2, 0.20 between points 2 and 3, -0.01 between points 3 and 4, and -0.19 between points 4 and 5.

### C. Applying weighting function to the transition phase

Applying the weighting functions on STS and GI to model the behavior of STW revealed that since the optimal value of  $\sigma$  was 0 the switch from STW behaving as STS to it behaving like GI occurs abruptly, and no gradual adaptation occurs. To further confirm this the same process was repeated on only the transition phase of STW. This was done to confirm that the transition phase in STW is comparable to the sensorimotor control phase that is observed in GI and that no part of it can be attributed to the preceding STS portion of the task. To do this the transition phase of GI and the rising/stabilizing

phase of STS were normalized to be the same length, and a weighting function was applied to each phase as described in the methods section. The optimal values for  $\mu$  and  $\sigma$  were found by minimizing the error between the model and the observed behavior of the STW transition phase. The results showed that the optimal values were  $\mu = 0$  (0 being the start of the transition/rising phase) and  $\sigma = 0$ . These values indicate that no part of the transition phase of STW can be attributed to STS influences and that the entire phase resembles the transition phase of GI more closely.